Spontaneous growth of Au nanoparticles onto electrodeposited CdSe thin film for plasmonic-enhanced photoelectrochemical water splitting

LIN CHEN, JIANPING LI[a], CHAOQUAN ZHOU, WENYUAN ZHU[a], HONGCHENG PAN[*]
College of chemistry and bioengineering, Guilin University of Technology, Guilin 541004, China
[a]Guangxi Key Laboratory of Electrochemical and Magnetochemical Function Materials, Guilin 541004, China

This article presents a simple method for fabrication of Au-CdSe thin films onto fluorine-doped SnO_2 (FTO) conducting glass substrates. The method starts with electrodeposition of CdSe thin films onto FTO substrates and followed by spontaneous growth of Au nanoparticles onto the CdSe surface in solutions containing $AuCl_4^-$ ions. X-ray diffraction (XRD), scanning electron microscopy (SEM), and energy dispersive X-ray (EDX) spectroscopy were used to investigate the Au-CdSe thin films. This work demonstrates that introducing plasmonic Au nanoparticles into photochemical reaction can substantially enhance the photo response to the solar splitting of water. The Au-CdSe/FTO photoelectrodes show an up to 7.5-fold enhancements of photocurrent density for photoelectrochemical water splitting, as compare to that of the bare CdSe/FTO electrode. The mechanisms of spontaneous growth of Au nanoparticles and plasmonic enhancement of the photocurrent are discussed.

(Received August 20, 2014; accepted November 13, 2014)

Keywords: CdSe, Au nanoparticles, Spontaneous growth, Plasmon, Water splitting

1. Introduction

Solar energy is by far the largest exploitable resource among renewable energy resources, providing more energy in 1 hour to the earth than all of the energy consumed by humans in an entire year [1]. Solar energy utilization requires effective means of capture, conversion, and storage of the solar radiation. Solar capture and conversion may be accomplished by photovoltaics. However, in the absence of cost-effective storage, solar electricity can never be a primary energy source for society. An especially attractive approach is to store solar-converted energy in the formation and breaking of chemical bonds, producing oxygen from water and a reduced fuel such as hydrogen, methane, methanol, or other hydrocarbon species.

Photoelectrochemical (PEC) water splitting is a promising approach to direct conversion of solar energy into storable hydrogen fuel that could act as a green energy carrier [2]. CdSe is an II-VI type semiconductor with a bulk direct band gap of 1.7 eV and high photosensitivity in the visible spectral region, which is employed in a number of optoelectronic devices such as PEC solar cells [3-6], photoconductors [7], and field-effect transistor [8]. Although bulk CdSe seems to have a suitable band position and a band gap with visible light response, it is not an active photocatalyst for water splitting [9]. Osterloh and co-workers demonstrated that photocatalytic hydrogen evolution from water can be achieved with CdSe nanoribbons in the presence of Na_2S/Na_2SO_3 as sacrificial electron donors and using ultraviolet or visible light [10]. They also found that when the CdSe nanoribbons are chemically linked to MoS_2 nanoplates, the photocatalytic activity increases almost four times [11]. CdSe, as a narrow band gap semiconductor, is used as a sensitizer to modify the wide band gap semiconductors (such as ZnO and TiO_2) for increasing their visible light absorption and improving the photocatalytic activities. For instance, Li et al. developed a doublesided CdS and CdSe quantum dots cosensitized ZnO nanowires arrayed photoanode for PEC hydrogen generation [12]. Also, they found that CdSe-sensitization and N-doping significantly enhances the PEC activities of TiO_2 nanostructured photoanodes [3].

Over the past several years, a new method for improving the efficiency of photocatalytic processes has emerged. This method introduces plasmonic materials into a photochemical reaction, which can markedly enhance the photo response to the solar water splitting. The mechanism of the enhancement may involve either charge transfer between metal and semiconductor (by so-called "hot" electron-hole pairs) or plasmon-induced heating and establishment of an electromagnetic field [13-19]. Liu and co-workers reported the preparation of three-dimensional porous CdSe films incorporated with plasmonic gold by the electrochemical layer-by-layer assembly [20]. The photovoltaic performance of CdSe photoanodes were

effectively enhanced by using plasmonic gold nanocrystals as light concentrators.

This work presents an alternative method for improving the performance of CdSe photoanodes for PEC water splitting by spontaneous growth of Au nanoparticles on the surface of CdSe thin film. The method is relatively simple and does not involve the addition of reducing agents.

2. Experimental details

2.1. Materials

$CdCl_2$ and SeO_2 were purchased from Sigma-Aldrich. $HAuCl_4{\cdot}4H_2O$ was purchased from Sinopharm (Shanghai, China). Cetyltrimethylammonium chloride (CTAC) was obtained from Beijing Chemical Reagent (Beijing, China). Other reagents were of analytical grade. Ultrapure water (resistivity>18 MΩ cm) was obtained from a WP-UP-IV-30 purification system (Woter, China) and used in the all experiments.

2.2. Electrodeposition of CdSe thin films

CdSe thin films were deposited on fluorine-doped SnO_2 (FTO) conducting glass substrates by electrochemical deposition technique. Electrodeposition was carried out on a CHI 660B electrochemical workstation (CH instruments, Shanghai, China) with a conventional three-electrode configuration consisted of a FTO glass slide (Xiangcheng technology, Guangzhou, China) as the working electrode, an Ag/AgCl (saturate KCl) reference electrode, and a Pt column auxiliary electrode. All potentials are reported versus the Ag/AgCl reference at room temperature. Before the electrodeposition, the FTO substrates were ultrasonically cleaned subsequently in ethanol, acetone, and water, followed by drying in air. CdSe thin films were deposited from aqueous solutions containing 25 mM $CdCl_2$ and 5 mM SeO_2. The electrodeposition was performed by potential cycling between -1.1 and 0 V for 50 cycles with a scan rate of 50 mV/s. The working electrode (hereinafter referred as CdSe/FTO) was then taken out, rinsed with ultrapure water, and dried in air, resulting in a dark orange-red film.

2.3 Growth of Au nanoparticles on CdSe/FTO slide

A 20-mL beaker was sequentially added with 9.55 mL of ultrapure water, 300 µL of 0.2 M phosphate buffer solution (PBS, pH 6.0), 100 µL of $HAuCl_4$ (1%, *w*/*w*), and 80 µL of 0.2 M CTAC. The CdSe/FTO slide was immersed in the above solution for a period of between 15 min and 3 h at 25°C. After the growth of Au nanoparticles, the electrode (hereinafter referred as Au-CdSe/FTO) was washed with ultrapure water and dried in air.

2.4 XRD, SEM, and photoelectrochemical measurements

The composition and structural properties of the Au-CdSe/FTO slides were studied by X-ray diffraction (X'pert PRO, Philips, Eindhoven, Netherlands). The morphologies of the Au-CdSe/FTO were directly subjected to characterize with a Hitachi S4800 field emission scanning electron microscope (Hitachi, Japan). Photocatalytic water splitting was performed in a side-window glass cell, using a 300 W Xe-lamp as the light source. Photoelectrochemical measurements were performed in a 0.24 M Na_2S + 0.35 M Na_2SO_3 solution with a three-electrode configuration consisting of a working electrode (CdSe/FTO or Au-CdSe/FTO slide), an Ag/AgCl reference electrode, and a platinum wire counter electrode at a potential scanning rate of 2 mV/s.

3. Results and discussion

A typical cyclic voltammogram (first cycle) for CdSe electrodeposition on FTO substrate is shown in Fig. 1. The curve displays a "nucleation loop" between the cathodic and anodic branches (from -0.45 to -0.84 V), which is indicative of the formation of CdSe nuclei on FTO substrate [7, 21]. In the weak acidic solution, H_2SeO_3 is formed through the reaction: $SeO_2 + H_2O \rightarrow H_2SeO_3$. Electrodeposition of CdSe is most likely to occur in two ways: 1) by reduction of H_2SeO_3 to H_2Se ($H_2SeO_3 + 6e^- + 6H^+ \rightarrow H_2Se + 3H_2O$), and then further reaction of H_2Se with Cd^{2+} takes place ($H_2Se + Cd^{2+} \rightarrow CdSe + 2H^+$), and 2) by direct reduction without the formation of an H_2Se intermediate ($H_2SeO_3 + Cd^{2+} + 6e^- + 6H^+ \rightarrow CdSe + 3H_2O$)[22-24]. On the reverse scan, one anodic peak at -0.35 V is related to the oxidation of cadmium ($Cd - 2e^- \rightarrow Cd^{2+}$) that had been formed in the initial negative sweep [7, 25].

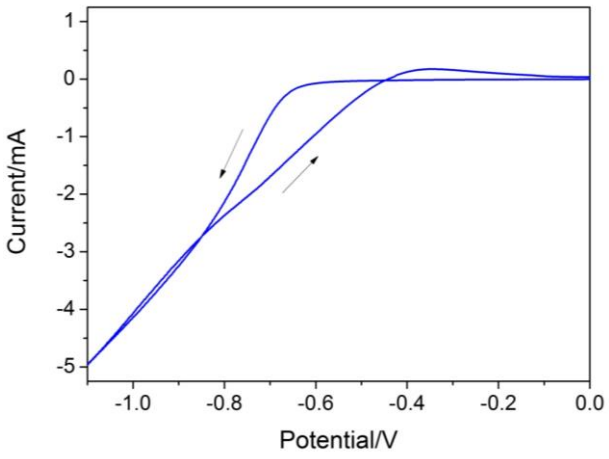

Fig. 1. Cyclic voltammogram of 25 mM $CdCl_2$ and 5 mM SeO_2 at 50 mV/s (vs Ag/AgCl reference).

The SEM micrograph (Fig. 2a and b) shows that the electrodeposited CdSe thin film is composed of the nanocrystalline spherical grains of an average size of ~22 nm. An XRD spectrum of the electrodeposited CdSe powder was obtained by scraping the film from the FTO substrate. The XRD pattern (Fig. 2c) reveals a face-centred cubic phase of CdSe (JCPDS 88-2346). The broad (111) diffraction peak at 2θ = 25.32° indicates the finite crystalline size of the CdSe crystals. The EDX analysis (Fig. 2d) shows that the atomic ratio of Cd/Se is 1.98, supporting a selenium-rich surface of CdSe/FTO. This indicates that the formation of elemental selenium competes with the formation of CdSe from H_2Se [7].

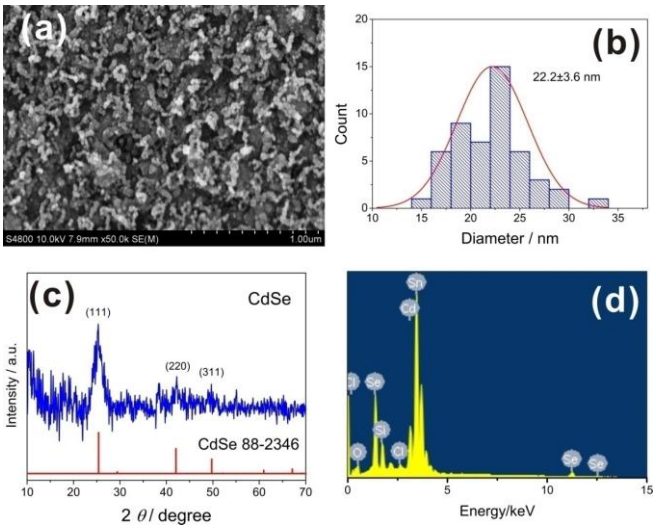

Fig. 2. (a) SEM micrograph, (b) the size distribution histogram, (c) XRD and (d) EDX of CdSe/FTO.

When the CdSe/FTO slide was immersed in a solution containing $HAuCl_4$, PBS, and CTAC, Au nanoparticles were deposited onto CdSe/FTO surface. Fig. 3a presents a typical SEM micrograph of the Au nanoparticles for deposition time of 3h. It can be seen that large nanoparticles were grown on the surface of CdSe/FTO. The size distribution histogram of the Au-CdSe/FTO is comprised of two groups of populations, one at about 21 nm, and the other at 45 nm. The first one can be attributed to CdSe nanoparticles, which is consistent with the average diameter of about 22 nm of the electrodeposited CdSe nanoparticles (Fig. 2a). We may reasonably conclude that the second one is attributed to grown Au nanoparticles. The XRD study confirm our conclusion that there are three diffraction peaks of 38.03°, 44.45°, and 64.61° at 2θ values indexed to (111), (200), and (220) the crystalline planes of the face-centered cubic structure of metallic gold (JPCDS 89-3697). Note that the peaks at 26.51°, 33.77°, 37.85°, 51.59°, 54.65°, 61.67°, and 64.49° derive from the FTO surface.

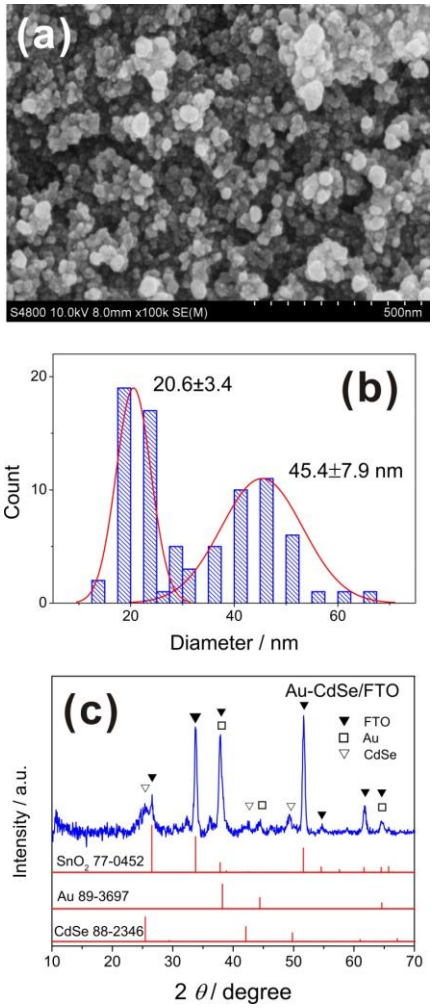

Fig. 3. (a) SEM micrograph, (b) the size distribution histogram and (c) XRD of Au nanoparticles grown on the surface of CdSe/FTO for 3 h.

The formation of Au nanoparticles may undergo adsorption and redox processes. It is well known that Au(III) ions are easily adsorbed onto the surface of sulfides via the strong Au–S bond. Recent studies show that the Au–Se bond is stronger than the corresponding Au–S bond by approximately 0.4 eV [26]. Therefore, we believe that $AuCl_4^-$ ions can be adsorbed onto CdSe surface. The $AuCl_4^-$ ions on the surface of CdSe can be immediately reduced to Au by selenide, because the standard reduction potential of $AuCl_4^-$/Au redox pair (1.002 V vs. the standard hydrogen electrode (SHE)) is higher than that of the Se/Se^{2-} (-0.924 V vs. SHE). The elemental gold should be mainly confined to the vicinity of the CdSe surface. Once the concentration of Au atoms has reached a critical value, they will nucleate and grow into small clusters, and eventually Au nanoparticles.

To investigate the effect of grown Au on the photocatalytic performance of CdSe thin film, the photoelectrochemical (PEC) performance of the

CdSe/FTO electrodes with different Au-grown time were studied under illumination with a 300 W Xenon lamp in the sulfide-sulfite (S^{2-}/SO_3^{2-}) aqueous electrolyte to suppress the photocorrosion of CdSe nanoparticles. Fig. 4 shows the photoresponsive anode current of the CdSe/FTO and Au-CdSe/FTO electrodes at a bias ranging from -0.6 V to 0.6 V (vs. Ag/AgCl) with light on-off cycles. The CdSe/FTO electrode yielded a relatively low photocurrent density of 0.14 mA/cm^2 at 0.365 V. The appearance of the anodic photocurrent indicates that the CdSe thin film functions as an n-type semiconductor. The photocurrent density of the CdSe/FTO electrode increased with growth time of Au nanoparticles (in the range of 0-1 h). The photocurrent density was enhanced after Au nanoparticles were grown on the electrode surface for 0.5 h (Fig. 4b). When the growth time of Au nanoparticles was increased to 1 h (Fig. 4c), the photocurrent density was enhanced by a factor of ~3.4, reaching 0.48 mA/cm^2 at 0.365 V. However, with the further increase of the growth time (3h), the photocurrent density of the Au-CdSe/FTO electrode was decreased (Fig. 4d).

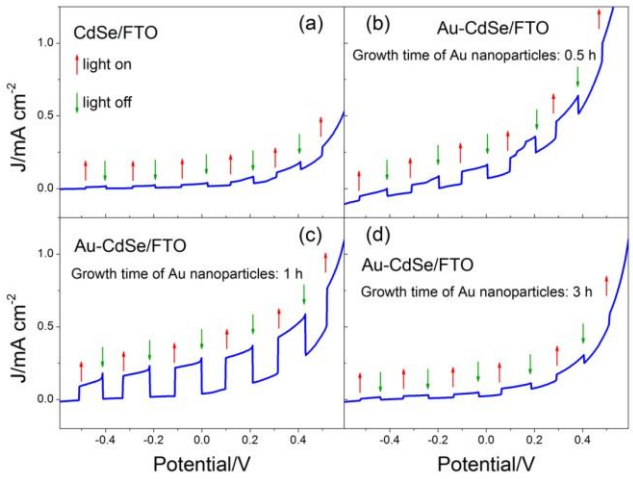

Fig. 4. Current–potential curves of the CdSe/FTO electrodes after growing Au nanoparticles for (a) 0, (b) 0.5, (c) 1 and (d) 3 h in an electrolyte of Na_2S/Na_2SO_3 solution under illumination with a chopped 300 W xenon lamp.

An amperometric study of the CdSe/FTO and Au-CdSe/FTO electrode was performed at a fixed bias of 0 V versus Ag/AgCl with on–off illumination cycles (Fig. 5). The obtained data are plotted in the form of a current–time curve in Fig. 4(b). A very low current of ~10^{-4} mA/cm^2 in the dark condition indicates that no chemical or electrochemical reaction of electrolysis occurred at the applied bias of 0 V under dark conditions. Upon illumination, the photocurrent density of the CdSe/FTO electrode quickly reached a stable value of 0.02 mA/cm^2, indicating a stable photoelectrolysis reaction occurred. The positive photocurrent indicates that the CdSe thin film acts as photoanode. The photocurrent density of the Au-CdSe/FTO electrodes is higher than that of CdSe/FTO electrode. The Au-CdSe/FTO prepared by grown Au nanoparticles for 1 h produced the highest photocurrent density of 0.15 mA/cm^2, which is approximately 7.5 times higher compare to that of the bare CdSe electrode. The enhancement of the photocurrent can be attributed to the formation of intense electric fields at the Au nanoparticle surface, which increase the rate of formation of electron/hole (e^-/h^+) pairs at the nearby CdSe particle surface [27]. The advantage of the formation of e^-/h^+ pairs near the CdSe semiconductor surface is that these charge carriers are readily separated from each other and easily migrate to the surface, where they can perform photocatalytic transformations. When the grown time of Au nanoparticles was further increased to 3 h, the photocurrent decreased and the enhancement effect was smaller. This photocurrent decrement may due to the quenching effect by the dense packing of Au nanoparticles, which is similar to those previously reported [28].

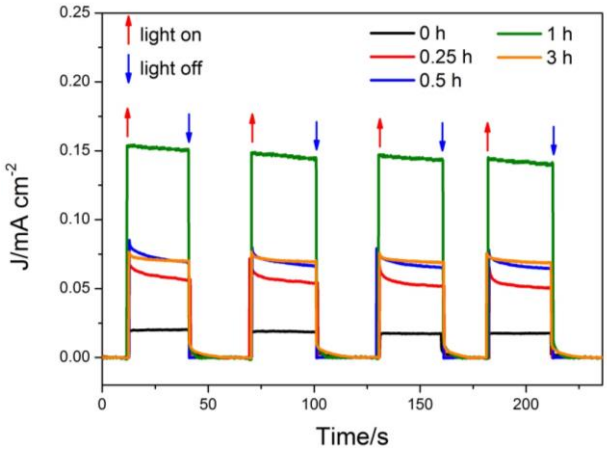

Fig. 5. Current–time curves of the CdSe/FTO electrodes with different growth time of Au nanoparticles held at 0 V in an electrolyte of Na_2S/Na_2SO_3 solution under illumination with a chopped 300 W xenon lamp.

4. Conclusions

In this paper, we have described a simple method for fabrication of Au-CdSe/FTO photoanodes. The method involves spontaneous growth of Au nanoparticles onto the surface of electrodeposited CdSe thin films. $AuCl_4^-$ ions can be adsorbed onto CdSe surface via the strong Au–Se bond. Because the standard reduction potential of $AuCl_4^-/Au$ redox pair is higher than that of the Se/Se^{2-}, the adsorbed $AuCl_4^-$ ions can be immediately reduced to Au nuclei. Finally, these Au nuclei grow into larger Au nanoparticles as more $AuCl_4^-$ ions were reduced. The Au-CdSe/FTO photoelectrodes show an up to 7.5-fold enhancements of photocurrent density for photoelectrochemical (PEC) water splitting, as compare to that of the bare CdSe electrode. The enhancement of the

photocurrent can be explained by the formation of intense electric fields at the Au nanoparticle surface, which increase the rate of formation of e^-/h^+ pairs at the nearby CdSe particle surface.

Acknowledgments

This work is supported by National Natural Science Foundation of China (20905016, 21265005) and Guangxi Natural Science Foundation (2013GXNSFBB053009).

References

[1] N. S. Lewis, D. G. Nocera, Proc. Natl. Acad. Sci. U. S. A., **103**, 15729 (2006).
[2] Y. Li, T. Takata, D. Cha, K. Takanabe, T. Minegishi, J. Kubota, K. Domen, Adv. Mater., **25**, 125 (2013).
[3] J. Hensel, G. Wang, Y. Li, J. Z. Zhang, Nano Lett., **10**, 478 (2010).
[4] K. Tarafder, Y. Surendranath, J. H. Olshansky, A. P. Alivisatos, L. W. Wang, J. Am. Chem. Soc., **136**, 5121 (2014).
[5] A. Kongkanand, K. Tvrdy, K. Takechi, M. Kuno, P.V. Kamat, J. Am. Chem. Soc., **130**, 4007 (2008).
[6] I. Gur, N. A. Fromer, M. L. Geier, A. P. Alivisatos, Science, **310**, 462 (2005).
[7] X. W. Gu, N. Shadmi, T. S. Yarden, H. Cohen, E. Joselevich, J. Phys. Chem. C, **116**, 20121 (2012).
[8] Z. He, W. Zhang, W. Zhang, J. Jie, L. Luo, G. Yuan, J. Wang, C. M. L. Wu, I. Bello, C.-S. Lee, S.-T. Lee, J. Phys. Chem. C, **114**, 4663 (2010).
[9] S. Kambe, M. Fujii, T. Kawai, S. Kawai, F. Nakahara, Chem. Phys. Lett., **109**, 105 (1984).
[10] F. Andrew Frame, E. C. Carroll, D. S. Larsen, M. Sarahan, N. D. Browning, F. E. Osterloh, Chem. Commun., 2206 (2008).
[11] F. A. Frame, F. E. Osterloh, J. Phys. Chem. C, **114**, 10628 (2010).
[12] G. Wang, X. Yang, F. Qian, J. Z. Zhang, Y. Li, Nano Lett., **10**, 1088 (2010).
[13] H. M. Chen, C. K. Chen, C.-J. Chen, L.-C. Cheng, P. C. Wu, B. H. Cheng, Y. Z. Ho, M. L. Tseng, Y.-Y. Hsu, T.-S. Chan, ACS Nano, **6**, 7362 (2012).
[14] H. M. Chen, C. K. Chen, R.-S. Liu, L. Zhang, J. Zhang, D. P. Wilkinson, Chem. Soc. Rev., **41**, 5654 (2012).
[15] S. Linic, P. Christopher, D. B. Ingram, Nat. Mater., **10**, 911 (2011).
[16] W. Hou, S. B. Cronin, Adv. Funct. Mater., **23**, 1612 (2013).
[17] P. Christopher, H. Xin, S. Linic, Nat Chem, **3**, 467 (2011).
[18] Z. Liu, W. Hou, P. Pavaskar, M. Aykol, S.B. Cronin, Nano Lett., **11**, 1111 (2011).
[19] A. Kubacka, M. Fernandez-Garcia, G. Colon, Chem. Rev., **112**, 1555 (2012).
[20] A. Liu, Q. Ren, M. Yuan, T. Xu, M. Tan, T. Zhao, W. Dong, W. Tang, Electrochim. Acta, **108**, 680 (2013).
[21] Y. Lai, F. Liu, J. Li, Z. Zhang, Y. Liu, J. Electroanal. Chem., **639**, 187 (2010).
[22] N. Shpaisman, U. Givan, F. Patolsky, ACS Nano, **4**, 1901 (2010).
[23] R. Mariappan, V. Ponnuswamy, S.M. Mohan, P. Suresh, R. Suresh, Mater. Sci. Semicond. Process., **15**, 174 (2012).
[24] J. Mallet, I. Kante, P. Fricoteaux, M. Molinari, M. Troyon, J. Solid State Electrochem., **16**, 1041 (2011).
[25] R. Henríquez, A. Badán, P. Grez, E. Muñoz, J. Vera, E. A. Dalchiele, R. E. Marotti, H. Gómez, Electrochim. Acta, **56**, 4895 (2011).
[26] S. Mankefors, A. Grigoriev, G. Wendin, Nanotechnology, **14**, 849 (2003).
[27] D. B. Ingram, S. Linic, J. Am. Chem. Soc., **133**, 5202 (2011).
[28] Y. Takahashi, S. Taura, T. Akiyama, S. Yamada, Langmuir, **28**, 9155 (2012).

*Corresponding author: hcpan@163.com